

Supporting Information

A comparative 2 and 4-probe DC and 2-Probe AC electrical conductivity of novel co-doped

$\text{Ce}_{0.9-x}\text{RE}_x\text{Mo}_{0.1}\text{O}_{2.1-0.5x}$ (RE = Y, Sm, Gd; x = 0.2, 0.3)

Qin Li and Venkataraman Thangadurai*

Department of Chemistry, University of Calgary, 2500 University Drive NW, Calgary, AB, T2N 1N4 Canada

* Correspondence E-mail: vthangad@ucalgary.ca. Tel.: 001 (403) 210 8649; Fax: 001 (403) 289 9488.

Table S1 The band gap from the diffuse reflectance spectra

Table S2 Fitting parameters of the impedance for $\text{Ce}_{0.6}\text{RE}_{0.3}\text{Mo}_{0.1}\text{O}_{1.95}$ (M = Sm, Gd) in air at 350 °C.

Table S3 Fitting parameters of the impedance for $\text{Ce}_{0.6}\text{RE}_{0.3}\text{Mo}_{0.1}\text{O}_{1.95}$ (RE = Sm, Gd) in air at 550 and 650 °C.

Table S4 Fitting parameters of the impedance for $\text{Ce}_{0.6}\text{RE}_{0.3}\text{Mo}_{0.1}\text{O}_{1.95}$ (RE = Sm, Gd) in air at 750 °C.

Fig. S1 PXRD patterns of (a) $\text{Ce}_{0.7}\text{Sm}_{0.2}\text{Mo}_{0.1}\text{O}_2$ (b) $\text{Ce}_{0.7}\text{Gd}_{0.2}\text{Mo}_{0.1}\text{O}_2$ and (c) $\text{Ce}_{0.7}\text{Y}_{0.2}\text{Mo}_{0.1}\text{O}_2$ prepared in air at elevated temperatures.

Fig. S2 Diffuse reflectance spectra of as prepared $\text{Ce}_{0.7}\text{Gd}_{0.2}\text{Mo}_{0.1}\text{O}_2$ and $\text{Ce}_{0.6}\text{Gd}_{0.3}\text{Mo}_{0.1}\text{O}_{1.95}$. For comparison, the starting materials are also given. Band value was estimated as described in ref. (65).

Fig. S3 FTIR spectra of as prepared $\text{Ce}_{0.7}\text{Gd}_{0.2}\text{Mo}_{0.1}\text{O}_2$ and $\text{Ce}_{0.6}\text{Gd}_{0.3}\text{Mo}_{0.1}\text{O}_{1.95}$. For comparison, the starting materials are also given.

Fig. S4 Scanning electron microscopy (SEM) images (10 μm) of as-prepared $\text{Ce}_{0.7}\text{RE}_{0.2}\text{Mo}_{0.1}\text{O}_2$ (a) = Sm; (b) = Gd and (c) = Y. Insets show the diagram at 20 μm . Their corresponding EDX images are given in (d) –(f).

Fig. S5 Typical AC resistivity plots of $\text{Ce}_{0.7}\text{Gd}_{0.2}\text{Mo}_{0.1}\text{O}_2$ and $\text{Ce}_{0.6}\text{Gd}_{0.3}\text{Mo}_{0.1}\text{O}_2$ at 350 °C in (a) air and (b) wet H_2 . Insets show the expanded view.

Fig. S6 Arrhenius plots for bulk electrical conductivity of (a) $\text{Ce}_{0.7}\text{Sm}_{0.2}\text{Mo}_{0.1}\text{O}_2$ (b) $\text{Ce}_{0.7}\text{Gd}_{0.2}\text{Mo}_{0.1}\text{O}_2$ and (c) $\text{Ce}_{0.7}\text{Y}_{0.2}\text{Mo}_{0.1}\text{O}_2$ in air and wet H_2 determined by 2-probe electrical measurements using Pt electrodes. About four to five orders of magnitude higher electrical conductivity was observed in wet H_2 . For comparison, 4-probe DC electrical conductivity data in wet H_2 was included.

Fig. S7 Powder X-ray diffraction patterns of (a) $\text{Ce}_{0.7}\text{Sm}_{0.2}\text{Mo}_{0.1}\text{O}_2$ (b) $\text{Ce}_{0.7}\text{Gd}_{0.2}\text{Mo}_{0.1}\text{O}_2$ and (c) $\text{Ce}_{0.7}\text{Y}_{0.2}\text{Mo}_{0.1}\text{O}_2$ after AC impedance measurement up to 700°C in wet H_2 .

Fig. S8 Powder X-ray diffraction patterns of (a) $\text{Ce}_{0.6}\text{Sm}_{0.3}\text{Mo}_{0.1}\text{O}_{1.95}$ (b) $\text{Ce}_{0.6}\text{Gd}_{0.3}\text{Mo}_{0.1}\text{O}_{1.95}$ and (c) $\text{Ce}_{0.6}\text{Y}_{0.3}\text{Mo}_{0.1}\text{O}_{1.95}$ after AC impedance measurement up to 700°C in wet H_2 .

Fig. S9 (a) Typical variation of electrical current as a function of time of $\text{Ce}_{0.6}\text{Gd}_{0.3}\text{Mo}_{0.1}\text{O}_{1.95}$ in wet H_2 at 450 °C for the 2- probe DC measurement with the applied potential of 0.1 V and 0.4 V. It demonstrates that an initial transient current converges on a steady-state current for an applied bias of 0.1 and 0.4 V at 450 °C. For clarity, we have shown both current and time in the log scale. A steady state current was observed within 1 Sec. In (b), we show the variation of voltage as a function of time for $\text{Ce}_{0.6}\text{Gd}_{0.3}\text{Mo}_{0.1}\text{O}_{1.95}$ in wet H_2 at 450 °C using the 4-probe DC measurement. A similar behavior was observed for the Sm and Y compounds.

Fig. S10 PXRD patterns showing the chemical stability of $\text{Ce}_{0.7}\text{Sm}_{0.2}\text{Mo}_{0.1}\text{O}_2$ with YSZ after sintering the reaction mixture (1:1 weight ratio) at (a) 1000°C, (b) 900°C and (c) 800°C in wet H_2 for 24 h. For comparison, (d) the mixture of $\text{Ce}_{0.7}\text{Sm}_{0.2}\text{Mo}_{0.1}\text{O}_2$ with YSZ, (e) the starting materials YSZ powders and (f) as-prepared $\text{Ce}_{0.7}\text{Sm}_{0.2}\text{Mo}_{0.1}\text{O}_2$ are shown. New phases due to Mo (JCPDS Card No 42- 1120) and $\text{Zr}_{0.4}\text{Ce}_{0.6}\text{O}_2$ (JCPDS Card No. 38-1439) are marked with * and #, respectively.

Table S1 Estimated band gap from the diffuse reflectance spectra

Composition	Eg (eV)	Literature values Eg (eV)
CeO_2	3.31	Present work 3.31, ⁶⁰ 3.1, ⁶¹ 3.55, ⁶² 3.19-(bulk) ⁶³ 3.15, ⁶⁴ 3.35 ⁶⁵
$\text{Ce}_{0.7}\text{Gd}_{0.2}\text{Mo}_{0.1}\text{O}_2$	3.07	Present work
$\text{Ce}_{0.6}\text{Gd}_{0.3}\text{Mo}_{0.1}\text{O}_{1.95}$	3.09	Present work
MoO_3	3.15	Present work 3.15 (polycrystalline thin film), ⁶⁶ 3.0-3.4 (amorphous film), ⁶⁷ 2.9 (bulk), ⁶⁸ 3.05, ⁶⁹ 3.16 (amorphous film), ⁷⁰ 3.27 (crystalline film) ⁷⁰

Table S2 Fitting parameters of the impedance for $\text{Ce}_{0.6}\text{RE}_{0.3}\text{Mo}_{0.1}\text{O}_{1.95}$ (M = Sm, Gd) in air at 350 °C.

Compound	Q1 (F)			Q2 (F)			Q3 (F)	
	R1 (Ω)	n1	C1(F)	R2 (Ω)	n2	C2 (F)	^a R3 (Ω)	n3
$\text{Ce}_{0.6}\text{Sm}_{0.3}\text{Mo}_{0.1}\text{O}_{1.95}$	6.73×10^3	6.09×10^{-10}	1.84×10^{-11}	1.69×10^5	1.40×10^{-7}	4.87×10^{-8}	2.77×10^{12}	5.79×10^{-5}
		0.78			0.78			0.26
$\text{Ce}_{0.6}\text{Gd}_{0.3}\text{Mo}_{0.1}\text{O}_{1.95}$	1.10×10^4	1.76×10^{-9}	2.59×10^{-11}	1.38×10^5	2.15×10^{-7}	5.85×10^{-8}	3.22×10^{14}	1.11×10^{-4}
		0.72			0.73			0.38

^aExtrapolated value.

Table S3 Fitting parameters of the impedance for $\text{Ce}_{0.6}\text{RE}_{0.3}\text{Mo}_{0.1}\text{O}_{1.95}$ (RE = Sm, Gd) in air at 550 and 650 °C.

Compound	T (°C)	Q2 (F)			Q3 (F)			Q4 (F)			
		R1 (Ω)	R2 (Ω)	n2	C2(F)	R3 (Ω)	n3	C3(F)	R4 (Ω)	n4	C4(F)
$\text{Ce}_{0.6}\text{Sm}_{0.3}\text{Mo}_{0.1}\text{O}_{1.95}$	550	1.84×10^2	3.60×10^2	1.06×10^{-6}	1.06×10^{-6}	1.52×10^3	2.14×10^{-5}	2.73×10^{-7}	7.38×10^3	2.46×10^{-3}	2.40×10^{-2}
				1.00			0.44			0.56	
$\text{Ce}_{0.6}\text{Gd}_{0.3}\text{Mo}_{0.1}\text{O}_{1.95}$	650	61.48	89.85	1.41×10^{-6}	8.79×10^{-7}	1.44×10^2	2.46×10^{-4}	8.33×10^{-7}	3.79×10^2	9.68×10^{-3}	2.69×10^{-2}
				0.95			0.37			0.56	
$\text{Ce}_{0.6}\text{Sm}_{0.3}\text{Mo}_{0.1}\text{O}_{1.95}$	550	2.31×10^2	3.25×10^2	2.02×10^{-6}	2.02×10^{-6}	1.18×10^3	2.26×10^{-5}	2.24×10^{-7}	7.33×10^3	1.78×10^{-3}	9.86×10^{-3}
				1.00			0.44			0.60	
$\text{Ce}_{0.6}\text{Gd}_{0.3}\text{Mo}_{0.1}\text{O}_{1.95}$	650	66.96	75.76	1.89×10^{-6}	1.07×10^{-6}	121.4	1.87×10^{-4}	6.40×10^{-7}	4.55×10^2	5.74×10^{-3}	1.26×10^{-2}
				0.94			0.40			0.55	

Table S4 Fitting parameters of the impedance for $\text{Ce}_{0.6}\text{RE}_{0.3}\text{Mo}_{0.1}\text{O}_{1.95}$ (RE = Sm, Gd) in air at 750 °C.

Compound	Q2 (F)			Q3 (F)			
	R1 (Ω)	R2 (Ω)	n2	C2(F)	R3 (Ω)	n3	C3(F)
$\text{Ce}_{0.6}\text{Sm}_{0.3}\text{Mo}_{0.1}\text{O}_{1.95}$	31.61	30.33	6.11×10^{-6}	5.41×10^{-7}	40.54	2.78×10^{-2}	3.41×10^{-2}
			0.78			0.37	
$\text{Ce}_{0.6}\text{Gd}_{0.3}\text{Mo}_{0.1}\text{O}_{1.95}$	32.76	29.81	9.94×10^{-6}	6.63×10^{-7}	41.95	1.51×10^{-2}	9.21×10^{-3}
			0.75			0.48	

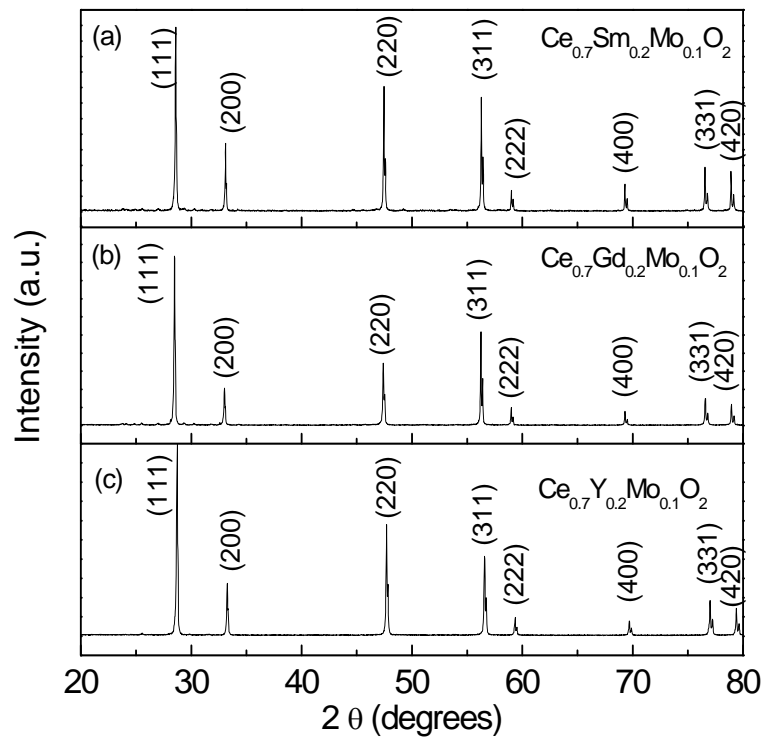


Fig. S1 PXRD patterns of (a) $\text{Ce}_{0.7}\text{Sm}_{0.2}\text{Mo}_{0.1}\text{O}_2$ (b) $\text{Ce}_{0.7}\text{Gd}_{0.2}\text{Mo}_{0.1}\text{O}_2$ and (c) $\text{Ce}_{0.7}\text{Y}_{0.2}\text{Mo}_{0.1}\text{O}_2$ prepared in air at elevated temperatures.

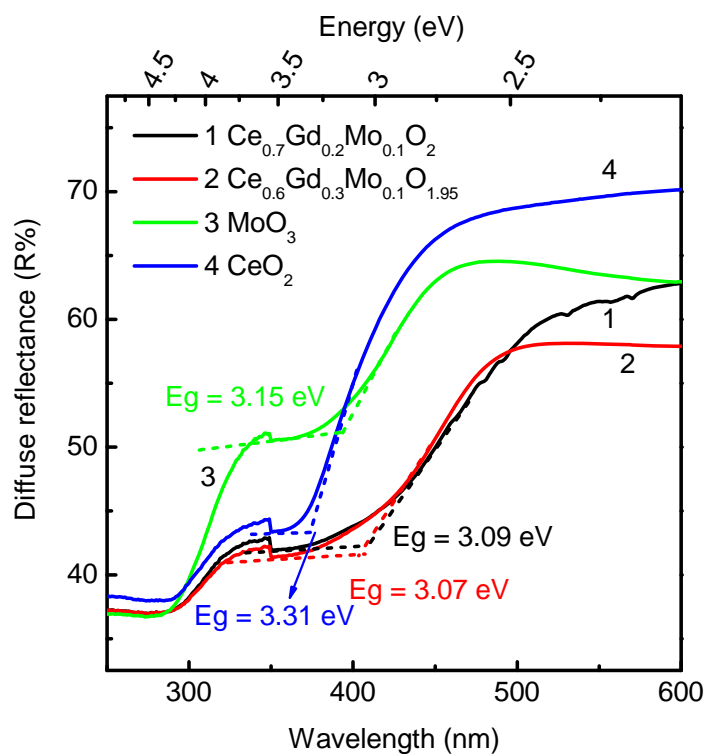


Fig. S2 Diffuse reflectance spectra of as prepared $\text{Ce}_{0.7}\text{Gd}_{0.2}\text{Mo}_{0.1}\text{O}_2$ and $\text{Ce}_{0.6}\text{Gd}_{0.3}\text{Mo}_{0.1}\text{O}_{1.95}$. For comparison, the starting materials are also given. Band value was estimated as described in ref. (65).

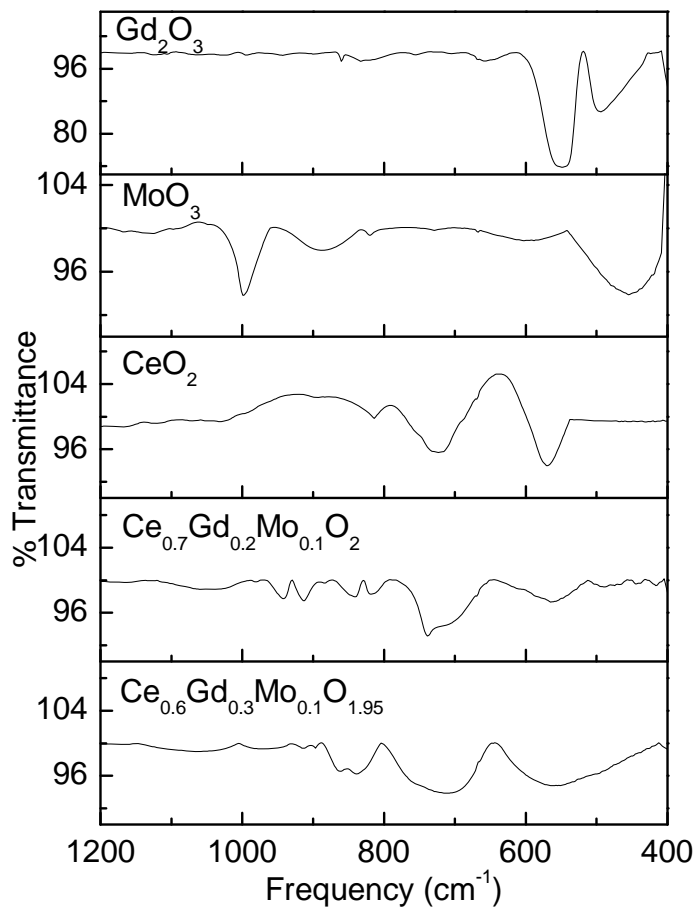


Fig. S3 FTIR spectra of as prepared $\text{Ce}_{0.7}\text{Gd}_{0.2}\text{Mo}_{0.1}\text{O}_2$ and $\text{Ce}_{0.6}\text{Gd}_{0.3}\text{Mo}_{0.1}\text{O}_{1.95}$. For comparison, the starting materials are also given.

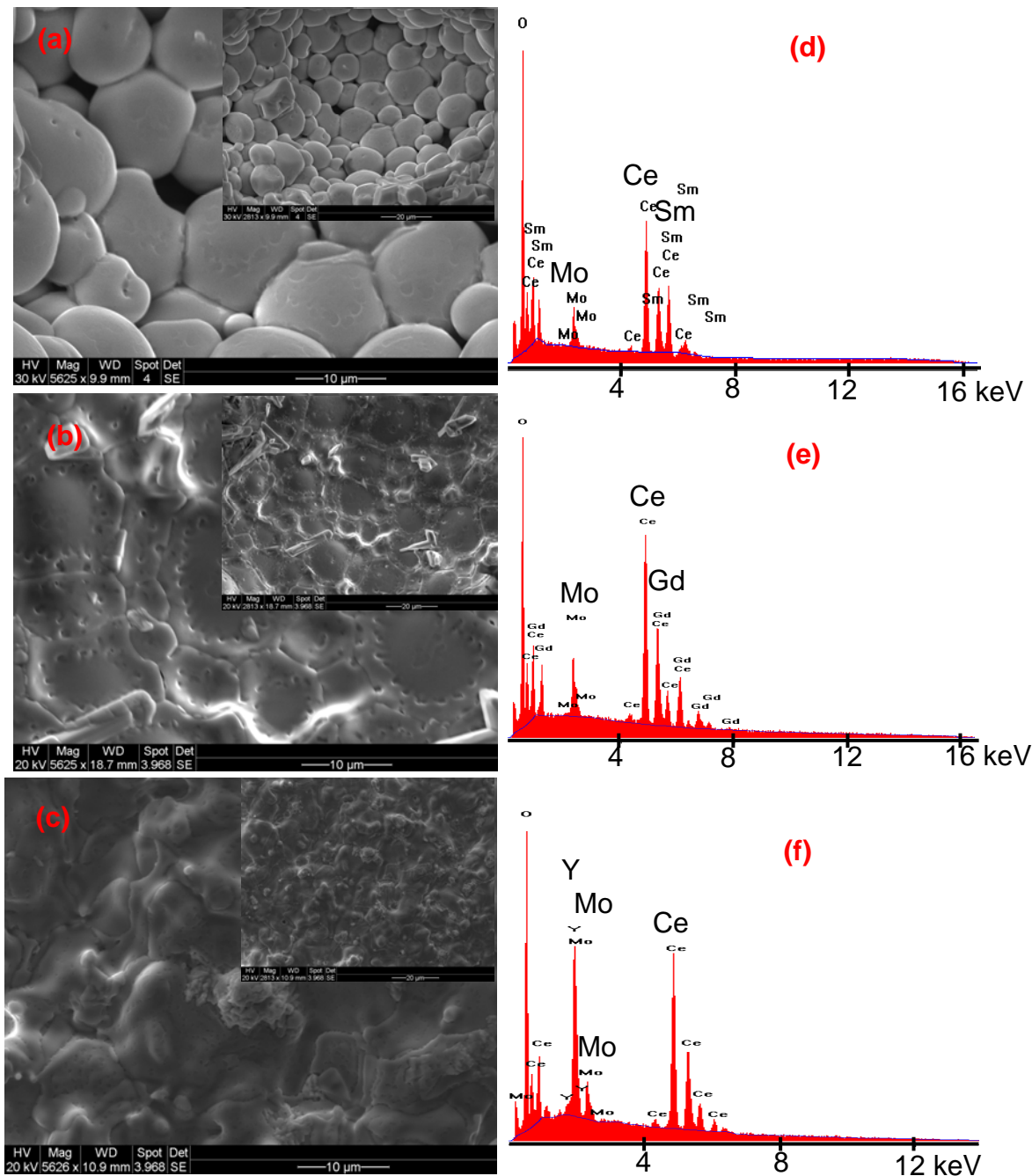


Fig. S4 Scanning electron microscopy (SEM) images (10 μm) of as-prepared Ce_{0.7}RE_{0.2}Mo_{0.1}O₂ (a) = Sm; (b) = Gd and (c) = Y. Insets show the diagram at 20 μm. Their corresponding EDX images are given in (d) – (f).

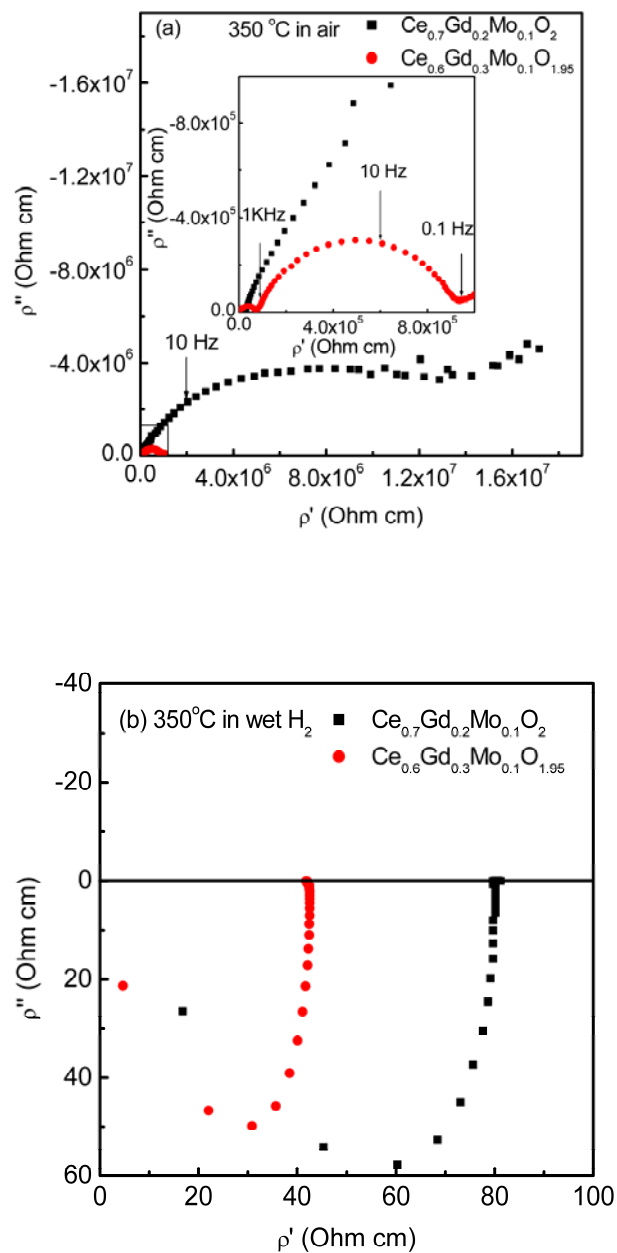


Fig. S5 Typical AC resistivity plots of $\text{Ce}_{0.7}\text{Gd}_{0.2}\text{Mo}_{0.1}\text{O}_2$ and $\text{Ce}_{0.6}\text{Gd}_{0.3}\text{Mo}_{0.1}\text{O}_{1.95}$ at $350\text{ }^{\circ}\text{C}$ in (a) air and (b) wet H_2 . Insets show the expanded view.

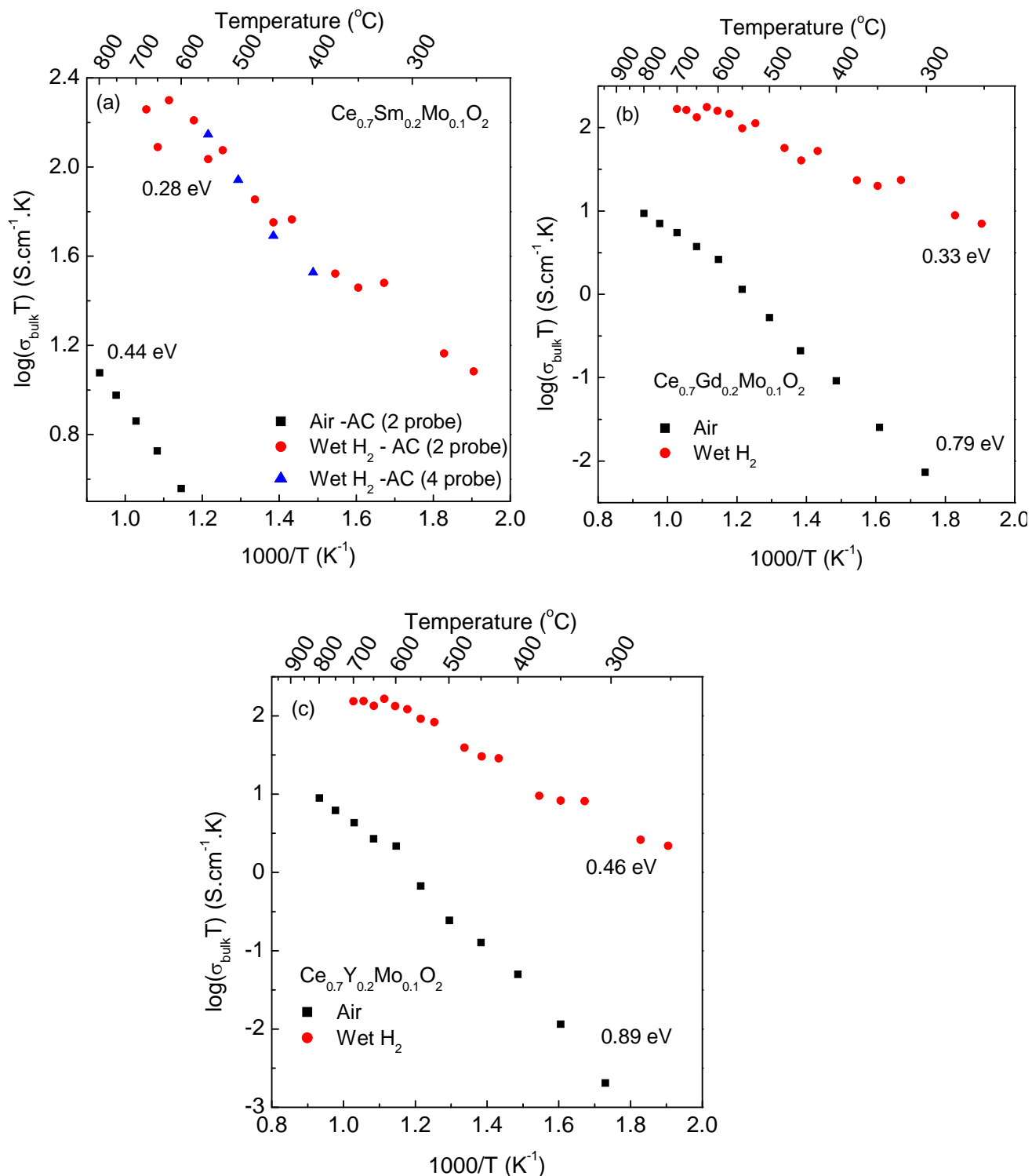


Fig. S6 Arrhenius plots for bulk electrical conductivity of (a) $\text{Ce}_{0.7}\text{Sm}_{0.2}\text{Mo}_{0.1}\text{O}_2$ (b) $\text{Ce}_{0.7}\text{Gd}_{0.2}\text{Mo}_{0.1}\text{O}_2$ and (c) $\text{Ce}_{0.7}\text{Y}_{0.2}\text{Mo}_{0.1}\text{O}_2$ in air and wet H_2 determined by 2-probe electrical measurements using Pt electrodes. About four to five orders of magnitude higher electrical conductivity was observed in wet H_2 . For comparison, 4-probe DC electrical conductivity data in wet H_2 was included.

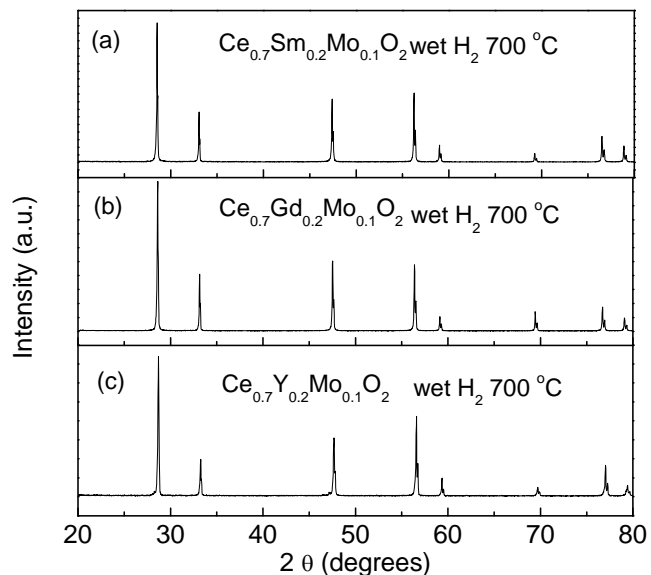


Fig. S7 Powder X-ray diffraction patterns of (a) $\text{Ce}_{0.7}\text{Sm}_{0.2}\text{Mo}_{0.1}\text{O}_2$ (b) $\text{Ce}_{0.7}\text{Gd}_{0.2}\text{Mo}_{0.1}\text{O}_2$ and (c) $\text{Ce}_{0.7}\text{Y}_{0.2}\text{Mo}_{0.1}\text{O}_2$ after AC impedance measurement up to 700°C in wet H_2 .

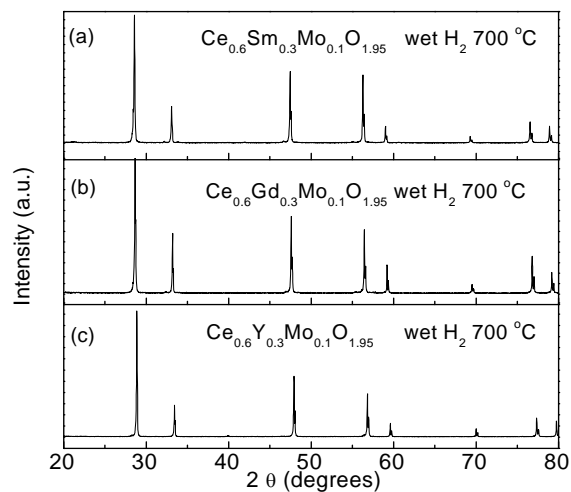


Fig. S8 Powder X-ray diffraction patterns of (a) $\text{Ce}_{0.6}\text{Sm}_{0.3}\text{Mo}_{0.1}\text{O}_{1.95}$ (b) $\text{Ce}_{0.6}\text{Gd}_{0.3}\text{Mo}_{0.1}\text{O}_{1.95}$ and (c) $\text{Ce}_{0.6}\text{Y}_{0.3}\text{Mo}_{0.1}\text{O}_{1.95}$ after AC impedance measurement up to 700°C in wet H_2 .

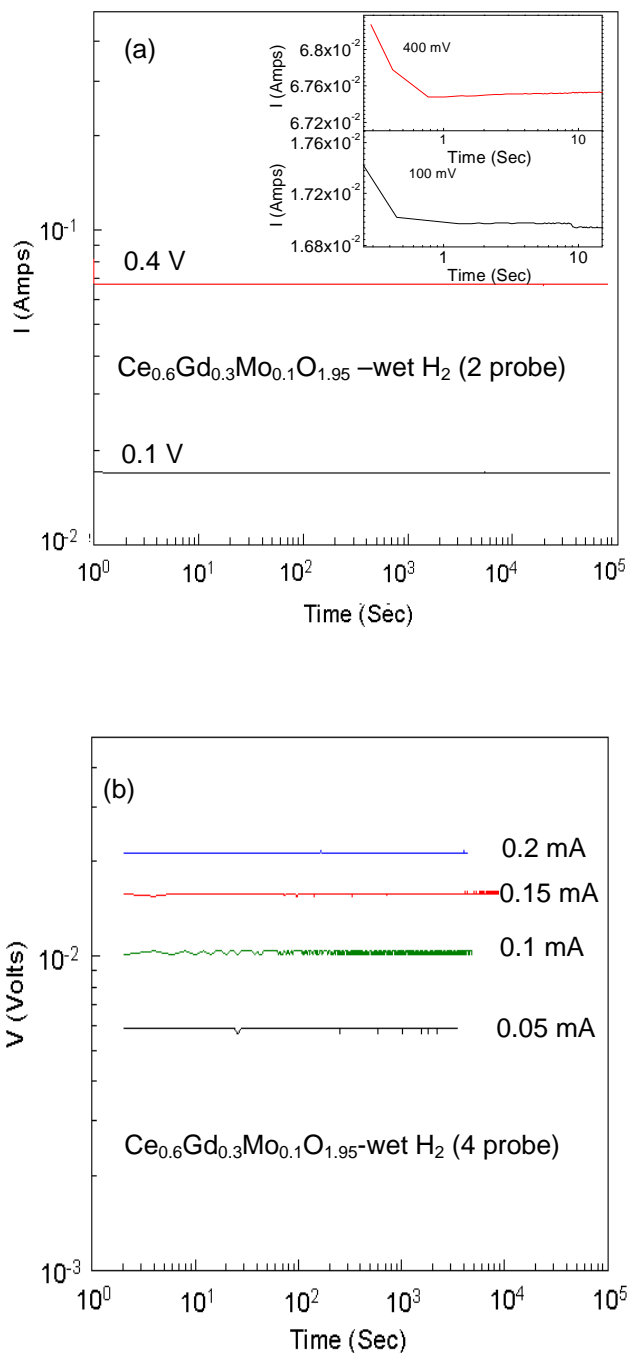


Fig. S9 (a) Typical variation of electrical current as a function of time of $\text{Ce}_{0.6}\text{Gd}_{0.3}\text{Mo}_{0.1}\text{O}_{1.95}$ in wet H_2 at 450 °C for the 2- probe DC measurement with the applied potential of 0.1 V and 0.4 V. It demonstrates that an initial transient current converges on a steady-state current for an applied bias of 0.1 and 0.4 V at 450 °C. For clarity, we have shown both current and time in the log scale. A steady state current was observed within 1 Sec. In (b), we show the variation of voltage as a function of time for $\text{Ce}_{0.6}\text{Gd}_{0.3}\text{Mo}_{0.1}\text{O}_{1.95}$ in wet H_2 at 450 °C using the 4-probe DC measurement. A similar behavior was observed for the Sm and Y compounds.

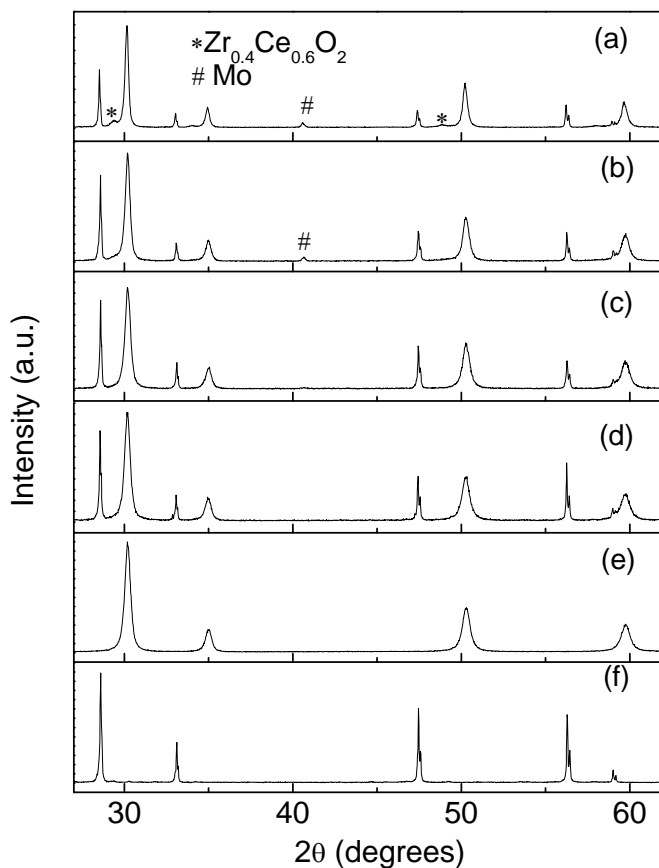


Fig. S10 PXRD patterns showing the chemical stability of $\text{Ce}_{0.7}\text{Sm}_{0.2}\text{Mo}_{0.1}\text{O}_2$ with YSZ after sintering the reaction mixture (1:1 weight ratio) at (a) 1000°C , (b) 900°C and (c) 800°C in wet H_2 for 24 h. For comparison, (d) the mixture of $\text{Ce}_{0.7}\text{Sm}_{0.2}\text{Mo}_{0.1}\text{O}_2$ with YSZ, (e) the starting materials YSZ powders and (f) as-prepared $\text{Ce}_{0.7}\text{Sm}_{0.2}\text{Mo}_{0.1}\text{O}_2$ are shown. New phases due to Mo (JCPDS Card No 42- 1120) and $\text{Zr}_{0.4}\text{Ce}_{0.6}\text{O}_2$ (JCPDS Card No. 38-1439) are marked with * and #, respectively.

References

- 60 S. Sathyamurthy, K. J. Leonard, R. T. Dabestani, and M. P. Paranthaman, *Nanotechnology* 2005, **16**, 1960.
- 61 A. Bensalem, G. Shafeev, and F. Bozon-Verduraz, *Catalysis Letters* 1993, **18**, 165.
- 62 D. E. Zhang, X. J. Zhang, X. M. Ni, J. M. Song, and H. G. Zheng, *Chem. Phys. Chem.* 2006, **7**, 2468.
- 63 F. Cheviré, C. Muñoz, C. F. Baker, F. Tessier, O. Larcher, S. Boujday, C. Colbeau-Justin, and R. Marchand, *J. Solid State Chem.* 2006, **179**, 3184.
- 64 T. V. Semikina, *Semiconductor Physics, Quantum Electronics & Optoelectronics*. 2004, **7**, 291.
- 65 T. Y. Ma, Z. Y. Yuan, and J. L. Cao, *Eur. J. Inorg. Chem.* 2010, 716.
- 66 C. Julien, O Mohammad Hussain, L. El-Farh, and M. Balkanski, *Solid State Ionics* 1992, **53-56**, 400.
- 67 M. Yahaya, M. M. Salleh, and I. A. Talib, *Solid State Ionics* 1998, **113-115**, 421.
- 68 T. Toyoda, H. Nakanishi, S. Endo, and T. Irie, *J. Phys. D: Appl. Phys.* 1985, **18**, 747.
- 69 Y. Zhao, J. G. Liu, Y. Zhou, Z. J. Zhang, Y. H. Xu, H. Naramoto, and S. Yamamoto, *J. Phys.: Condens. Matter.* 2003, **15**, L547.
- 70 T. S. Sian and G. B. Reddy, *Solar Energy Materials and Solar Cells* 2004, **82**, 375.